Photoluminescence of $CsPbCl_3$ films prepared by quench deposition and subsequent heat treatments

2003 J. Phys.: Condens. Matter 15 1247

(http://iopscience.iop.org/0953-8984/15/8/309)

INSTITUTE OF PHYSICS PUBLISHING JOURNAL OF PHYSICS: CONDENSED MATTER

J. Phys.: Condens. Matter **15** (2003) 1247–1257 PII: S0953-8984(03)53009-0

Photoluminescence of $CsPbCl_3$ films prepared by quench deposition and subsequent heat treatments

S Kondo[1], H Nakagawa[2], T Saito[1] and H Asada[3]

[1] Research Centre for Development of the Far-Infrared Region, Fukui University, Bunkyo, Fukui 910-8507, Japan
[2] Department of Electronics, Faculty of Engineering, Fukui University, Bunkyo, Fukui 910-8507, Japan
[3] Department of Applied Physics, Faculty of Engineering, Fukui University, Bunkyo, Fukui 910-8507, Japan

Received 4 September 2002
Published 17 February 2003
Online at stacks.iop.org/JPhysCM/15/1247

Abstract

Photoluminescence spectra of $CsPbCl_3$ have been measured for various (nano-, micro-, and poly-) crystalline states, using film samples of high quality achieved by quench deposition and subsequent heat treatments. In great contrast to the case for bulk $CsPbCl_3$, all the spectra are characterized by a single, free-exciton emission band, exhibiting no emission related to trap states even for the microcrystalline/nanocrystalline states. The microcrystalline/nanocrystalline states show much stronger free-exciton emission than the polycrystalline state. The enhanced free-exciton emission is suggestive of the occurrence of excitonic superradiance. The absence of trap states is favourable for excitonic superradiance.

1. Introduction

Several papers have been published on the photoluminescence of $CsPbCl_3$ crystals. Different luminescence spectra have been observed for $CsPbCl_3$ excitons, depending on the different crystalline forms (or morphologies) of the specimens studied. Basically three distinct emission bands show up for the bulk $CsPbCl_3$ crystal [1–4], namely that due to a free exciton and those due to two kinds of trapped exciton, whereas for the polycrystalline $CsPbCl_3$ film [5], the emission due to trapped excitons is weak in intensity and unresolved in structure, as compared with the free-exciton emission. On the other hand, various features of exciton emission bands appear for microcrystals embedded in a CsCl crystal matrix [6–8], depending on the sample preparation methods.

It has been shown that many metal halides such as silver [9], thallium [10], copper [11], lead [12], and cadmium [13] halides, including their mixed systems [14], can be rendered amorphous by quench deposition yielding film samples. The amorphous films exhibit excellent transmittance below the absorption edge and have a well defined, characteristic

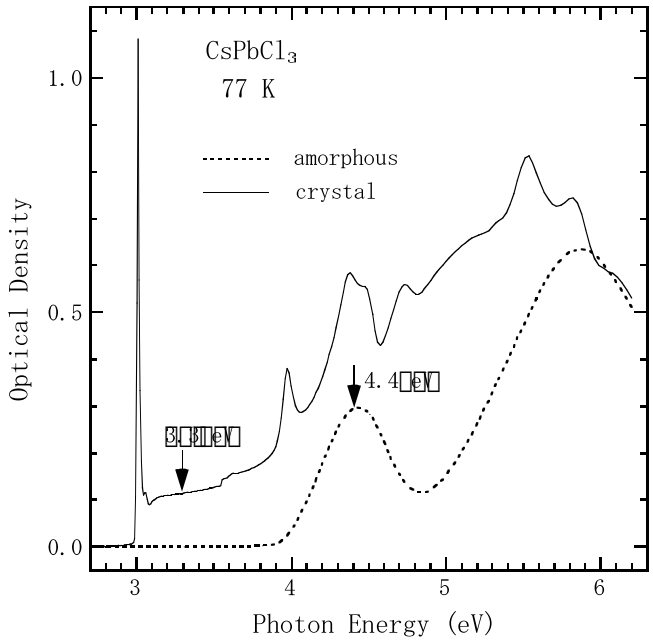

Figure 1. The absorption spectra at 77 K for the amorphous (dashed curve) and crystalline (solid curve) states. The downward-pointing arrows indicate the energy positions of the luminescence-exciting lights used.

crystallization temperature at which their absorption spectra drastically change in outline. The films, when crystallized at temperatures just above the crystallization temperature, are generally in a microcrystalline state, and change into the polycrystalline state when they are subsequently annealed at higher temperatures. Many of the crystalline films produced via the amorphous phase, whether they are microcrystalline or polycrystalline in nature, show very high transmittance compared with (polycrystalline) films deposited onto hot substrates. These properties of the films are particularly evident for $CsPbCl_3$. This motivates the present studies. We are interested in two questions: which emission bands are dominant for the excitons in such high-quality $CsPbCl_3$ films; and what modification is exhibited in the luminescence spectrum due to the effect of confinement of the excitons within the microcrystallites in the films?'

$CsPbCl_3$ is characterized by very different (by 1 eV) optical energy gaps for the amorphous (4 eV) and the crystalline (3 eV) states, with the latter showing a sharp exciton absorption peak just above the gap (figure 1). This is favourable for investigating absorption and/or luminescence properties of $CsPbCl_3$ microcrystals embedded in the amorphous matrix of the same compound. (Completely crystallized) microcrystalline films, on the other hand, provide alternative, extremely densely microcrystal-dispersed, specimens (of a filling factor of unity for the $CsPbCl_3$ microcrystal particles) for studies of mesoscopic optical properties of microcrystals. In the present work, we measured the luminescence, as well as absorption, spectra for the amorphous, microcrystalline (or nanocrystalline), and polycrystalline states of the same starting $CsPbCl_3$ films prepared by quench deposition.

2. Experimental details

The amorphous films of $CsPbCl_3$ were obtained by quench deposition onto silica-glass substrates attached to a copper block cooled to 77 K. The deposition was carried out in a

vacuum of about 9×10^{-6} Pa using a tungsten basket heating element placed 8 cm in front of the substrate [12]. The crystallization (into a microcrystalline state) of the amorphous films and subsequent crystal growth (into a polycrystalline state) in the films were carried out in two different ways, i.e., by a rapid heating/cooling operation (rapid heating up to above the crystallization temperature, 302 K [15], immediately followed by rapid cooling to 77 K) and a slow heating/cooling operation. The former operation was performed by means of shot-like IR irradiation of the films using a cw CO_2 laser (wavelength, 10.6 μm; power, 10 W), with the substrate kept in contact with the 77 K copper block. One shot caused one cycle of the rapid heating/cooling. The irradiation time per shot was in the range 10^{-2}–3 s, depending on the desired crystalline sizes. On the other hand, the latter operation was carried out by heating the copper block with a resistive heater, at the heating rate 10 K min^{-1} (the cooling rate was in the range 10–50 K min^{-1}). For each run of the rapid or slow heating/cooling cycles, photoluminescence and absorption spectra of the films were measured *in situ* using a liquid nitrogen-cooled CCD spectrometer equipped with a 0.47 m grating monochromator. A 500 W xenon lamp (in combination with a 0.5 m grating monochromator) and a 30 W deuterium lamp were used as the light sources for the photoluminescence and absorption measurements, respectively. The luminescence was excited at 4.4 and 3.3 eV (downward-pointing arrows in figure 1) for the amorphous and crystalline states, respectively, and recorded in a backward-scattering geometry to minimize reabsorption. The recorded luminescence spectra were not corrected for spectral sensitivity of the measuring system. The CCD element itself had a relatively flat spectral sensitivity in the region 3800–7900 A (3.26–1.57 eV).

3. Results and discussion

Figures 2 and 3 show the luminescence spectra at 77 K of a quench-deposited $CsPbCl_3$ film for the amorphous (figure 2), microcrystalline (figure 3(a), dashed curve), and polycrystalline (figure 3(a), solid curve) states, together with the absorption spectra (at 77 K) for the microcrystalline (figure 3(b), dashed curve) and polycrystalline (figure 3(b), solid curve) states. The spectra were first measured for the as-deposited (amorphous) film, and then the film was subjected to the first and second runs of the slow heating/cooling operation to measure the spectra for the microcrystalline and polycrystalline states, respectively. The highest temperature (annealing temperature) experienced by the film and its time duration (annealing time) were, respectively, 350 K and 10 min for the first run (microcrystalline state) and 450 K and 10 min for the second run (polycrystalline state).

As seen from figure 2, three emission bands were observed for the amorphous state, namely a prominent band peaking at around 2.85 eV (with a full width at half-maximum, FWHM, of about 0.5 eV) and two small bands at 2.50 and 1.92 eV, with the 1.92 eV band superimposed on a broad, weak emission band around 1.8 eV. These bands were characterized by very large Stokes shifts, e.g., about 1.58 eV for the highest-energy (2.85 eV) emission band, relative to the first absorption band peaking at 4.4 eV (excitation energy; see figure 1).

Previously [12], we discussed the absorption spectrum of amorphous $CsPbCl_3$ in terms of a molecular orbital theory based on a localized quasicomplex $Pb^{2+}(Cl^-)_6$ model, where the 4.4 eV absorption band was related to the spin–orbit allowed $^3P_1$ excited state produced by the transitions from the localized Pb^{2+} 6s–6p states. The consideration was recently confirmed by our subsequent measurement [16] of the fundamental absorption spectrum of (crystalline) Cs_4PbCl_6, whose crystal structure is composed of a hexagonal regular array of $Pb^{2+}(Cl^-)_6$ octahedra with the central Pb^{2+} ions mutually isolated by intervening (between the octahedra) Cs^+ ions, and whose low-energy absorption characteristics were very similar in feature to those of the amorphous $CsPbCl_3$. As compared with the above-presented emission spectrum

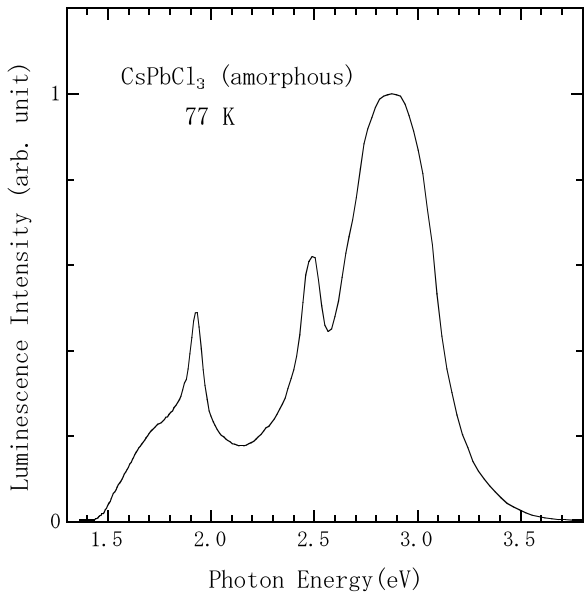

Figure 2. The luminescence spectrum measured at 77 K for the amorphous state using the 4.4 eV exciting light.

(figure 2) of the amorphous $CsPbCl_3$, however, the spectrum of crystalline Cs_4PbCl_6 excited at 4.3 eV (peak energy of the lowest absorption band) exhibits a prominent emission band at around 3.4 eV (FWHM, 0.36 eV) with the Stokes shift 0.9 eV [5], at liquid nitrogen temperature. It is interesting to note that, despite the close resemblance of the absorption properties of the amorphous $CsPbCl_3$ and crystalline Cs_4PbCl_6, they show quite different luminescence properties from each other. For disclosing the origin of the difference, however, detailed measurements are necessary.

For the crystalline states (figure 3(a))—microcrystalline or polycrystalline—only a single emission band due to exciton recombination was observed (no other emission was observed although the measurements were carried out over the photon energy region down to 1.4 eV). Its peak energy and FWHM were, respectively, 3.019 eV and 22 meV for the microcrystalline state and 3.005 eV and 19 meV for the polycrystalline state. The corresponding exciton absorption peak energies were 3.021 and 3.014 eV, respectively, yielding very small Stokes shifts (2 and 9 meV, respectively). The confinement-induced blue-shift of the exciton energy was larger for the emission energy (14 meV) than for the absorption energy (7 meV). It should be noted that the exciton luminescence was strongly enhanced in intensity by the confinement of the exciton, as seen from the comparison of the two emission bands in figure 3(a); the ratio of their peak intensities amounted to 2.1.

The present exciton luminescence is different in feature from any $CsPbCl_3$ exciton luminescence reported so far, i.e., for bulk $CsPbCl_3$ crystals [1–4], polycrystalline $CsPbCl_3$ films [5], and $CsPbCl_3$ aggregates in Pb^{2+}-doped CsCl crystals [6–8]. For example, the luminescence spectrum of the bulk crystal measured at liquid nitrogen temperature [2] is composed of three bands, peaking at 2.987, 2.950, and 2.914 eV with the integrated intensity ratio of about 1:2:0.4 (which was deduced in [2] from the measured spectrum by a line-shape analysis using Gaussian fits). The highest-energy band is attributed to free excitons and the lower-energy bands to trapped excitons. At lower temperatures below 40 K, the free-exciton

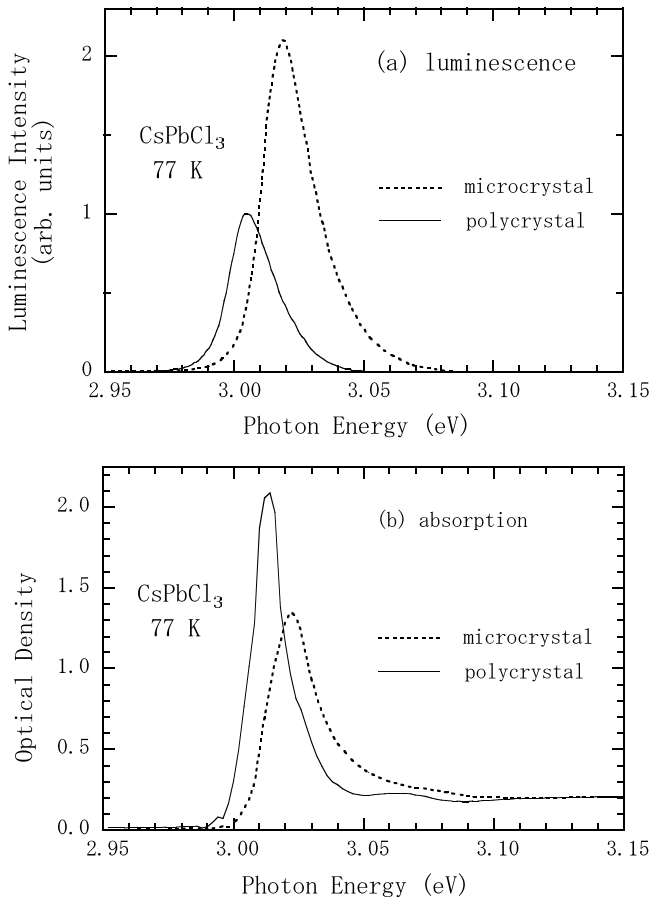

Figure 3. The luminescence (a) and absorption (b) spectra measured at 77 K for the microcrystalline (dashed curves) and polycrystalline (solid curves) states. The luminescence was excited at 3.3 eV.

luminescence becomes strongest in intensity. The FWHM of the free-exciton luminescence band is almost the same (70–80 meV) in the temperature range at and below liquid nitrogen temperature. For polycrystalline films [5], a free-exciton emission band (peak energy, 2.960 eV; FWHM, about 30 meV) was observed at 5 K together with weaker lower-energy emission due to trapped excitons. For Pb^{2+}-doped CsCl crystals, complicated structural emission spectra [6, 7] were observed, depending on the different ways in which the specimens were heat-treated. The structural character was interpreted in terms of plate-like growth of the $CsPbCl_3$ aggregates (in a suitably heat-treated sample, several emission bands were observed due to recombination of the free excitons confined in various $CsPbCl_3$ plates with different thicknesses). On the other hand, the present luminescence spectra are composed of a single, free-exciton emission band with higher peak energies (3.005 and 3.019 eV for polycrystalline and microcrystalline states, respectively) and smaller FWHMs (19 and 22 meV, respectively). There are no trap states for the excitons in the films prepared by crystallization via the amorphous phase. It is considered that lattice imperfections such as impurities and lattice distortions are driven away from the interior of the individual crystallites in the crystallized film. It is notable that excitons even in the microcrystalline film are free from being trapped, despite the expectation of a high density of surface states.

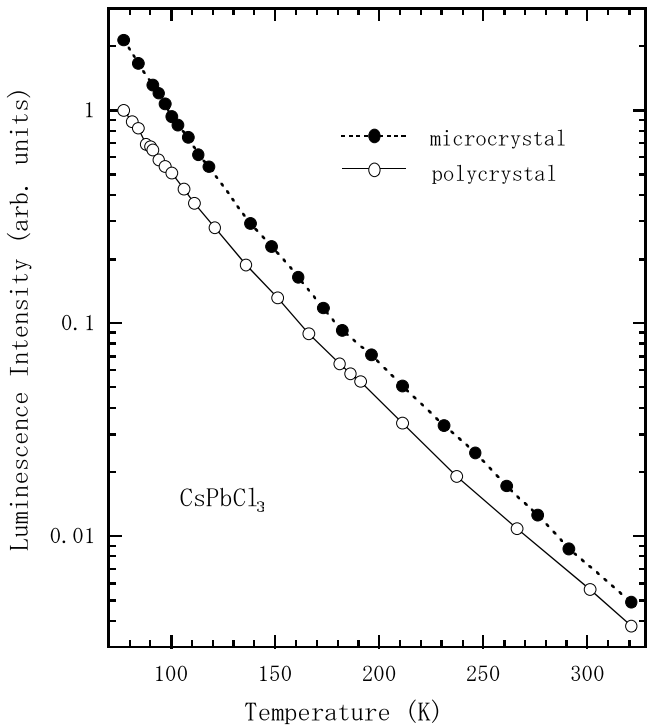

Figure 4. The temperature dependence of the peak intensity of the luminescence excited at 3.3 eV, measured for the microcrystalline (solid circles) and polycrystalline (open circles) states.

Figure 4 shows the temperature dependence of the exciton luminescence, where the peak intensities of the emission bands are plotted logarithmically versus temperature. The luminescence was distinctly observed even at room temperature for both the microcrystalline and polycrystalline states. The activation energy was roughly estimated to be in the range 40–120 meV for both states. The values are favourably compared with the binding energies, 60–67 meV [15, 17, 18], of the $CsPbCl_3$ excitons. The quenching of the luminescence with increasing temperatures is attributable to ionization of the free excitons.

To investigate confinement-enhanced free-exciton luminescence for various crystalline sizes, we observed luminescence spectra stepwise during nucleation and subsequent crystal growth in a quench-deposited $CsPbCl_3$ film. For this purpose, we monitored the luminescence spectra, together with the absorption spectra, of the film subjected to repeated cycles of the rapid heating/cooling operation described in the previous section. The results are shown in figure 5. The numbers, 1–7, in the figure indicate the orders of the runs of the heating/cooling cycle. For larger numbers (run numbers), both the luminescence (figure 5(a)) and the absorption (figure 5(b)) spectra shifted to lower energies. On the other hand, although the absorption intensity monotonically increased with the run number, the luminescence was maximum in intensity for the third run (run number 3), after which the luminescence intensity decreased with increasing run number. Notably the absorption intensity was much weaker for the third run than for the last run (number 7); the last run was characterized by the biggest absorption peak and the weakest luminescence band. It was shown that the integrated (up to 4 eV) absorption intensity below 4 eV (where the $CsPbCl_3$ film was transparent in the amorphous state) remained almost unchanged after the third run, indicating completion of the film crystallization at the third run.

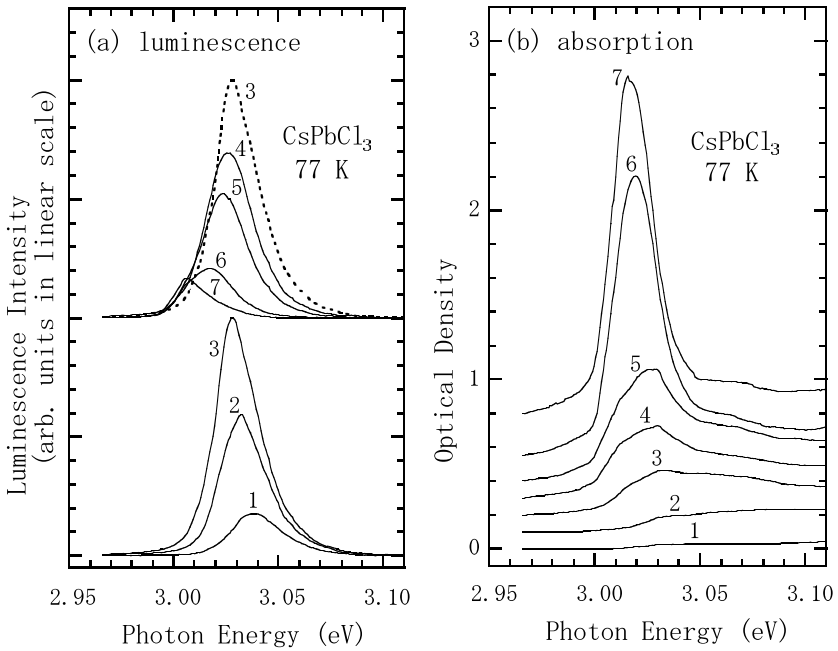

Figure 5. The sequential change of the luminescence (a) and absorption (b) spectra due to rapid heating/cooling cycles (see the text). The spectra are differently shifted along the *y*-axis for clarity. The luminescence was excited at 3.3 eV.

The FWHM of the luminescence band decreased with the run number from 28 meV (first run) to 18 meV (last run). It is notable that the luminescence spectrum for every crystalline state was invariably composed of a single, free-exciton emission band with larger peak energies (3.005–3.038 eV) and smaller FWHMs (18–28 meV) than those reported so far for the $CsPbCl_3$ bulk and film samples.

The peak energies of both the exciton emission (3.006 eV) and absorption (3.016 eV) spectra for the last run are very close to those (3.005 and 3.014 eV, respectively) of the polycrystalline film shown in figure 3. The resulting film (after the last run) is, therefore, considered to be nearly in the polycrystalline state. The substantially blue-shifted spectra appearing in the earlier stages of the rapid heating/cooling cycles reflect the microcrystalline or nanocrystalline nature of the film. It is considered that fine microcrystallites of $CsPbCl_3$ were generated in the amorphous surroundings in the first and second runs and a microcrystalline film (with a filling factor of unity for the $CsPbCl_3$ microcrystal particles) was yielded in the subsequent runs. Thus the crystal growth from microcrystal/nanocrystal to polycrystal occurred stepwise in the film during the period from the first to the last heating/cooling cycles. We note here that the emission band for the microcrystalline state achieved by the slow heating/cooling cycle (figure 3(a)) was situated, in its peak energy (3.019 eV) and peak intensity (2.1 times that for the polycrystalline state), between the emission bands for the fifth (peak energy, 3.024 eV; peak intensity, 3.2 times that for the last run) and sixth (3.016 eV; 1.3 times) runs in figure 5(a).

To compare the luminescence efficiency (by which we mean the luminescence intensity per net crystalline film thickness) among different crystalline sizes, we first normalized the luminescence spectra in figure 5(a) with respect to the absorbed intensity of the exciting light (figure 6(a)) and then corrected the results for reabsorption (figure 6(b)). In the correction for

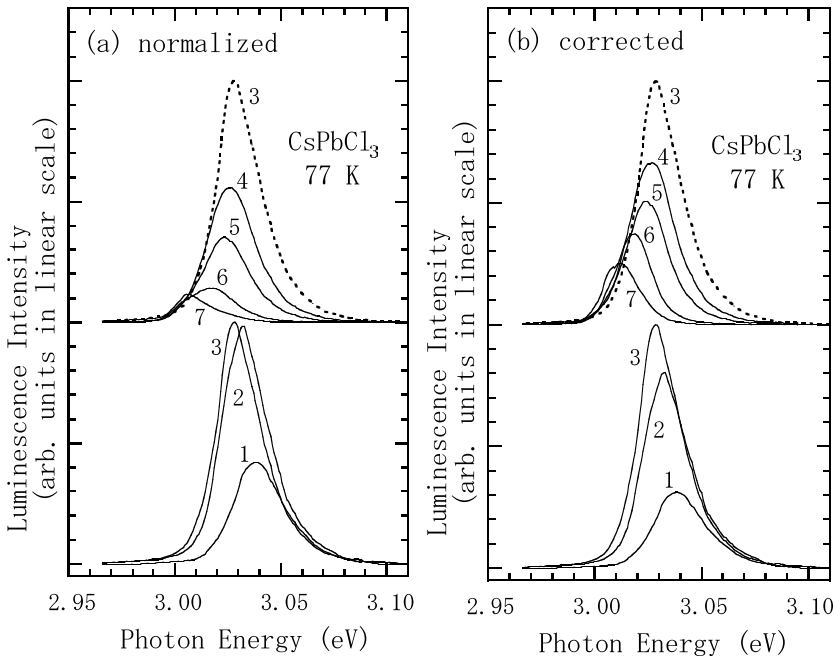

Figure 6. The sequential change of the luminescence spectrum, normalized (a) with respect to the absorbed intensity of the exciting light (3.3 eV) and then corrected (b) for reabsorption.

reabsorption, we assumed an exponential decrease inside the film of the exciting light, and neglected the effect of the subsequent reabsorption of the re-emitted light because the efficiency of emission at 77 K was considered to be low (as compared to 'expected' lower-temperature efficiencies; see figure 4). Thus the correction was made using the relation

$$I_{cor}(h\nu) \propto \frac{[\alpha(h\nu) + \alpha(h\nu_{exc})]I_{nor}(h\nu)}{(1 + \exp\{-[\alpha(h\nu) + \alpha(h\nu_{exc})]d\}}, \tag{1}$$

where $I_{nor}(h\nu)$ is the normalized emission intensity, shown in figure 6(a), of the film excited at $h\nu_{exc}$ (3.3 eV) measured at photon energy $h\nu$. $\alpha(h\nu)$ and $\alpha(h\nu_{exc})$ are the absorption coefficients of the film at $h\nu$ and $h\nu_{exc}$, respectively, and d is its thickness. As seen from the figure, the larger the run number, the stronger the effect of the correction; the peak intensity for the last run (polycrystalline state) was enhanced by a factor of 2.9 by the correction. Nevertheless the luminescence efficiency was smallest for the polycrystalline state.

For quantitative comparison of the luminescence intensities among different crystalline sizes, we plotted, in figure 7, the integrated intensities of the corrected luminescence spectra versus the blue-shifts in peak energies relative to the peak energy for the polycrystalline state; all the data points are indicated by the run numbers. The x-axis of the plot can be viewed as a measure of the mean size of the crystallites in the film—that is, the larger the x-value, the smaller the size. It is seen from the figure that the microcrystalline state with the 17 meV blue-shift is enhanced in luminescence efficiency by a factor of 5.2 compared to the polycrystalline state.

A possible explanation for the microcrystallite-size dependence of the luminescence intensity may be given in terms of excitonic superradiance. Excitonic superradiance is a cooperative radiation process of a coherently delocalized exciton in a crystal, leading to a very short radiative decay time depending on the coherence length, i.e., the extent of the coherently

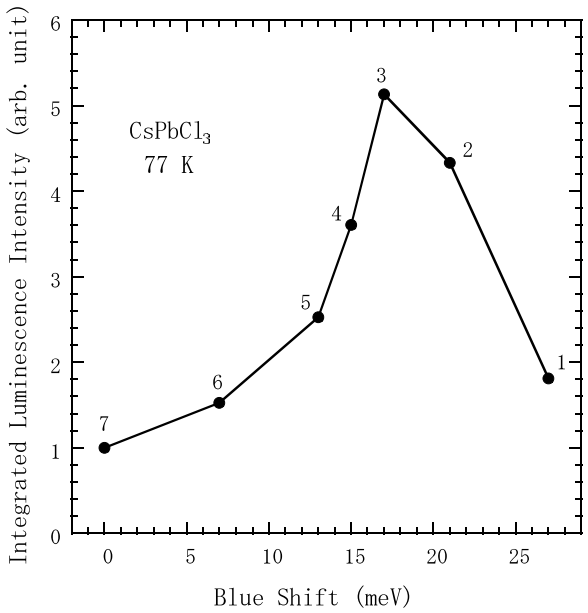

Figure 7. The integrated luminescence intensities of the corrected luminescence spectra shown in figure 6(b) plotted versus the blue-shift in peak energy relative to the peak energy for the polycrystalline state.

delocalized exciton. Since the coherently delocalized exciton state is the coherent superposition of all the lowest electronic excited states at individual unit cells contained in the crystal, such an ideal state is generally not achieved in a bulk crystal due to lattice imperfection (as well as lattice vibration) even at very low temperatures. However, the situation is different in the case of a very small crystallite (microcrystal), because the exciton coherence length is limited to the size of the crystallite and thus because the exciton can easily be coherently delocalized throughout the crystallite. Therefore, excitonic superradiance has only been observed for microcrystals of high quality (review articles are available [19, 20]).

Nikl *et al* [8] observed picosecond decay kinetics of the $CsPbCl_3$ aggregates (microcrystals) embedded in CsCl crystals. They found single-exponential decay with a decay time in the range 20–40 ps at 10 K for the free-exciton emission. They ascribed the very short decay time (compared with that observed for the bulk-crystal free-exciton emission, about 500 ps at 10 K [2]) to excitonic superradiance in the $CsPbCl_3$ aggregates. It is quite reasonable to assume that the superradiance-induced very rapid radiative decay causes a very high luminescence yield of the confined excitons. Therefore, it is tempting to explain the luminescence behaviours (figure 7) in the present film in terms of excitonic superradiance, since the fact that there is no trap state in the film is favourable to excitonic superradiance (trap states may cause dephasing of excitonic superradiance). Indeed, in the luminescence spectrum for the $CsPbCl_3$ aggregates for which excitonic superradiance was reported [8], no emission bands due to trapped excitons were observed (such aggregates were achieved in a suitably heat-treated sample).

It is known that the decay time of the superradiant excitons is inversely proportional to the volume of the microcrystals [21, 22]. This means that the larger the size of the microcrystals, the higher the luminescence yield (per volume of the microcrystals), unless the excitonic superradiance is quenched. Therefore, under the assumption of excitonic superradiance in our

films, the increase of the luminescence intensity from run number 1 to run number 3 in figure 7 corresponds to the increase of the superradiance-enhanced radiative decay rate due to crystal growth. The subsequent decrease of the luminescence intensity with increasing run number, i.e., increasing size of the microcrystals in the film, is considered to be due to dephasing-induced quenching of the excitonic superradiance. The main cause of the dephasing in the excitonic superradiance may be exciton–phonon scatterings rather than lattice imperfections in the microcrystals. Preliminary measurements at liquid helium temperature showed intense free-exciton luminescence for larger microcrystals, presumably due to excitonic superradiance. The results will be reported elsewhere.

4. Conclusions

Photoluminescence spectra of $CsPbCl_3$ have been measured for various (nano-, micro-, and poly-) crystalline states, using film samples of high quality which can be achieved by quench deposition and subsequent heating/cooling operation. All the spectra exhibit a single, free-exciton emission band, without showing trapped-exciton emission, and thus reflecting a high-quality crystalline nature of individual crystallites in the films, in great contrast to the case for bulk $CsPbCl_3$ crystals. The microcrystalline/nanocrystalline states show much stronger free-exciton emission than the polycrystalline state. The enhanced free-exciton emission is suggestive of the occurrence of excitonic superradiance. The absence of the trap states is favourable to the assumption of excitonic superradiance. Excitonic superradiance of such extremely densely dispersed microcrystals as those in the $CsPbCl_3$ microcrystalline films is fascinating when considering application in thin-film lasers. Work is in progress aimed at achieving lasing action in such films. The results will be reported later.

References

[1] Nitsch K, Dusek M, Nikl M, Polak K and Rodova M 1995 *Prog. Cryst. Growth Charact.* **30** 1
[2] Nikl M, Mihokova E, Nitsch K, Polak K, Rodova M, Dusek M, Pazzi G P, Fabeni P, Salvini L and Gurioli M 1994 *Chem. Phys. Lett.* **220** 14
[3] Pashuk P, Pidzyrailo N S and Matsko M G 1981 *Sov. Phys.–Solid State* **23** 1263
[4] Amitin L N, Anistratov A T and Kuznetsov A L 1979 *Sov. Phys.–Solid State* **21** 2041
[5] Somma F, Aloe P and Lo Mastro S 2001 *J. Vac. Sci. Technol.* b **19** 2237
[6] Aceves R, Babin V, Barboza-Flores M, Fabeni P, Nikl M, Nitsch K, Pazzi G P, Perez Salas R and Zazubovich S 2001 *Phys. Status Solidi* b **225** 247
[7] Nikl M, Nitsch K, Polak K, Mihokova E, Zazubovich S, Pazzi G P, Fabeni P, Salvini L, Aceves R, Barboza-Flores M, Perez Salas R, Gurioli M and Scacco A 1997 *J. Lumin.* **72–74** 377
[8] Nikl M, Nitsch K and Polak K 1995 *Phys. Rev.* B **51** 5192
[9] See for example
Gottwald H G, Lieser T, Weil K G and Weiss Z 1985 *Z. Naturf.* A **40** 677
[10] See for example
Kondo S, Itoh T, Saito T and Mekata M 1991 *Solid State Commun.* **78** 557
[11] See for example
Gottwald H G and Weil K G 1988 *Ber. Bunsenges. Phys. Chem.* **92** 60
[12] See for example
Kondo S, Sakai T, Tanaka H and Saito T 1998 *Phys. Rev.* B **58** 11401
[13] See for example
Kondo S, Kagawa S and Saito T 1996 *Phys. Status Solidi* b **154** 583
[14] See for example
Kondo S, Amaya K and Saito T 2001 *Mater. Sci. Eng.* B **88** 85
[15] Kondo S, Mori H and Saito T 1997 *Phys. Status Solidi* a **163** 445
[16] Kondo S, Amaya K and Saito T 2001 *J. Phys. Soc. Japan* **70** 3751
[17] Fröhlich D, Heidelich K, Kunzel H, Trendel G and Treush J 1979 *J. Lumin.* **18/19** 385

[18] Pashuk I P, Pidzyrailo N S and Matsko G 1981 *Sov. Phys.–Solid State* **23** 1263
[19] Misawa K, Nomura S and Kobayashi T 1993 *Optics of Semiconductor Nanostructures* ed F Hennenberger, S Schmitt-Rink and E Göbel (Berlin: Akademie) pp 447–95
[20] Gaponenko S V 1998 *Optical Properties of Semiconductor Nanocrystals* (Cambridge: Cambridge University Press) pp 117–33
[21] Hanamura E 1988 *Phys. Rev.* B **38** 1228
[22] Itoh T, Furumiya M and Ikehara T 1990 *Solid State Commun.* **73** 271